A Fuzzy-Based Spatial Condition Detection System Using Square Area Mapping to Support the Mobility of Individuals with Visual Impairments

Tata Supriyadi
Department of Electrical Engineering, Politeknik Negeri Bandung, Bandung, Indonesia

Ridwan Solihin
Department of Electrical Engineering, Politeknik Negeri Bandung, Bandung, Indonesia

Endang Habinuddin
Department of Electrical Engineering, Politeknik Negeri Bandung, Bandung, Indonesia

Sudrajat Sudrajat
Department of Electrical Engineering, Politeknik Negeri Bandung, Bandung, Indonesia

TB. Utomo
Department of Electrical Engineering, Politeknik Negeri Bandung, Bandung, Indonesia

Tri Hartono
Department of Electrical Engineering, Politeknik Negeri Bandung, Bandung, Indonesia

Budi Setiadi
Department of Electrical Engineering, Politeknik Negeri Bandung, Bandung, Indonesia

Ramdhan Nugraha
PhD Student Department of Corvergence Engineering, Kumoh National Institute of Technology, Gumi, South Korea

Abstract: This study presents the development, design, and implementation of a smart cane prototype capable of recognising spatial environments to assist individuals with visual impairments in navigating obstacle-free paths. The system utilises a non-contact, non-visual electronic sensing mechanism based on ultrasonic technology. Ultrasonic sensors are strategically mounted at three positions on the cane—left, centre, and right (L, C, R). As the cane is swung from side to side, each sensor

Correspondents Author:
Tata Supriyadi, Department of Electrical Engineering, Politeknik Negeri Bandung, Indonesia
Email: tata.supriyadi@polban.ac.id

Received July 2 2025; Revised July 27, 2025; Accepted August 1, 2025; Published August 2, 2025.

continuously collects distance measurements, which are then averaged to provide a representative reading for each direction. These average distances are further processed into geometric estimations known as the Left Side Square Area (LSSA) and Right-Side Square Area (RSSA), serving as fuzzy logic inputs. A rule-based fuzzy inference system computes decisions, followed by a defuzzification stage executed within a microcontroller to determine appropriate responses. The outcomes are conveyed to the user via audio (beep) and tactile (vibration) feedback. Experimental trials involving visually impaired participants across two mobility scenarios demonstrated that the system effectively supports indoor navigation and serves as a viable prototype for orientation and mobility (O&M) training with modern travel aid applications.

Keywords: Stick, spatial identification, mobility of the visual mpairments, fuzzy-square area, sound and vibration cues

Introduction

Based on global data released by the World Health Organisation (WHO) in 2022, approximately 2.2 billion people worldwide suffer from some degree of visual impairment, including blindness. Notably, around 1 billion of these cases are classified as preventable or treatable, with the potential to restore near-normal vision through appropriate medical interventions (Bhatlawande et al., 2024; Organization, 2024; Tian et al., 2021; Zhang et al., 2023). In Indonesia, data from the Ministry of Health reveal that cataracts remain the leading cause of blindness among individuals aged 50 years and above. This finding is supported by the Rapid Assessment of Avoidable Blindness (RAAB) survey conducted between 2014 and 2016. Cataracts contribute to roughly 81% of the total population affected by visual impairments, which is estimated at around 8 million individuals. Among them, approximately 1.6 million are completely blind, while the remaining 6.4 million experience moderate to severe vision loss (Kementerian Kesehatan Republik Indonesia, 2021).

Visual impairment is characterised by a severe limitation or loss of visual perception. To achieve independent movement despite the inability to visually perceive spatial and environmental cues, individuals with visual impairments rely on O&M skills. Orientation refers to the cognitive ability to interpret one's environment—such as recognising landmarks, auditory cues, or tactile markers—using residual senses with or without assistive technology. This process enables the formation of mental maps to facilitate autonomous activity. In contrast, mobility focuses on the physical capability to move from one location to another

using non-visual sensory inputs and, if necessary, assistive devices to ensure safe and directed travel (Chundury et al., 2022; Ogedengbe et al., 2025).

This study presents an assistive technology in the form of a conventional white cane enhanced with a detachable electronic module. The system is designed to provide real-time navigational support for individuals with visual impairments by detecting obstacles such as walls and surrounding objects. The key innovation lies in the refinement of the detection algorithm previously introduced in (Supriyadi et al., 2024), which relied on direct input from left and right ultrasonic sensors. In contrast, the proposed system utilises a novel approach by calculating rectangular spatial areas from sensor data as input variables for a fuzzy logic-based decision-making algorithm. The final output is delivered to the user through a combination of audio beeps and tactile vibrations, offering intuitive and immediate feedback to support safe and efficient mobility.

Numerous studies have explored the development of electronic assistive technologies aimed at supporting the independent mobility of individuals with visual impairments. These technologies generally fall into three primary categories: (1) wearable haptic devices attached to various parts of the body, (2) robotic systems that function as intelligent surrogates for human guides or guide dogs, and (3) handheld solutions, commonly realised as smart canes. The underlying technologies range across contact and non-contact modalities, incorporating both visual and non-visual sensors such as cameras, sonar, infrared, Inertial Measurement Units (IMUs), Global Positioning Systems (GPS), and visible light sensors.

Wearable sensor-based systems are primarily designed to substitute visual input with tactile or auditory feedback through body-mounted devices. For instance, camera modules can monitor the spatial positioning of a user's arm relative to surrounding obstacles. This visual data is processed using deep learning techniques like Fast Region-based Convolutional Neural Networks (Fast R-CNN) to trigger tactile responses such as vibrations (Lee et al., 2023). The processed image data is translated into directional motor commands—e.g., prompting arm rotation to the left or right—to assist users in avoiding detected barriers (Barontini et al., 2021). Additionally, images of pedestrian and vehicular traffic signals can be analysed to activate both sound and vibration alerts (Tian et al., 2021). Some systems combine computer vision, ultrasonic sonar (Qiu et al., 2020), and GPS data (Bhatlawande et al., 2024) to enhance obstacle detection, distance estimation, and geolocation, with outputs delivered via vibration patterns to guide user movement (Kleinberg et al., 2023).

Robotic assistive systems treat robots as autonomous guides equipped with a suite of integrated sensors. These typically include vision-based cameras, infrared-based LiDAR, and GPS modules. Object detection and environmental mapping are executed through deep

learning algorithms, often employing YOLOv5 datasets, which process image and spatial data captured by the sensors. Navigation goals are tracked via GPS, and real-time feedback on movement and obstacle avoidance is conveyed to users through haptic (vibration) signals (Zhang et al., 2023).

Handheld assistive technologies, particularly in the form of advanced smart canes, often combine multiple sensor types—such as cameras, ultrasonic sonar, infrared lasers, LiDAR, GPS-GSM modules, and visible light detectors—to enhance navigational capabilities. These devices typically relay audio information to the user via Bluetooth-connected headsets (Jivrajani et al., 2023). Visual data captured through onboard cameras are analysed using YOLO and TensorFlow-based deep learning frameworks (Masud et al., 2022). Distance-based obstacle detection is performed through ultrasonic sensors, often integrated with servo motors for dynamic scanning (Cardillo et al., 2022). IMU sensors are also employed to monitor hand grip orientation and cane-swing motion, transmitting motion data to the headset in real-time (Tanabe et al., 2023). For multi-point navigation, GPS coordinates are processed using the haversine formula to calculate accurate distances, with the results communicated as auditory cues (Supriyadi et al., 2021). A notable innovation includes the implementation of LED transmitters installed at pedestrian crosswalks. These transmitters embed audio signals into visible light using Visible Light Communication (VLC). When the cane's photodiode receiver detects the VLC signal, the information is wirelessly transmitted to the user's headset (Darlis et al., 2024).

Research Method

This study adopts a hybrid research methodology that combines simulation and practical experimentation to develop a spatial orientation system tailored for individuals with visual impairments. The system's design requires a systematic selection of materials, hardware components, and suitable engineering methods. At its core, the system processes distance array data obtained from ultrasonic sensors, which are then transformed into geometric representations known as left and right square areas. These spatial measurements serve as the basis for generating real-time feedback in the form of audio signals and vibrations to assist user navigation. The development workflow encompasses several key stages: designing the external casing, assembling the electronic circuitry, and implementing the embedded software. The software component includes algorithms for square-area computation and decision-making using fuzzy logic principles.

Box Mechanics

The mechanical design of the device enclosure was developed using Autodesk Fusion 360. The casing comprises multiple interlocking components that can be manually assembled without requiring additional tools or fasteners, as depicted in Figure 1. Its primary function is to securely house the entire electronic system, including all hardware modules, and it is designed to be mounted onto a standard white cane.

The enclosure consists of four essential parts: the main housing, a locking mechanism, a detachable cover, and a sensor mounting bracket, as illustrated in Figure 1(a). The design is ambidextrous, featuring index finger grips on both sides to accommodate both right- and left-handed users. These grips enhance control and stability during lateral cane swings while ensuring that the sensors remain properly orientated forward.

To enhance accessibility, the enclosure includes tactile indicators that help visually impaired users distinguish various functional components by touch. Specific design elements include a recessed charging port for safe cable connection, a touch-sensitive menu and volume control area marked by an indented circular symbol, a raised power switch (ON/OFF) for quick identification, a sliding slot mechanism that locks the enclosure onto the cane, a snap-fit latch securing the cover in place, and a sensor holder with three fixed mounting positions.

The fully assembled enclosure is shown in Figure 1(b). The design adheres to the World Health Organisation (WHO) recommendations regarding weight limits, ergonomic function, and user-centred identity. The total weight of the enclosure is kept below 300 grams, with the empty shell weighing approximately 83 grams. Positioned at the upper end of the cane, the device maintains the core functionalities of traditional O&M techniques while preserving the visual identity of the cane as an assistive mobility tool.

Electronic Hardware

The design and implementation of electronic hardware to support O&M for individuals with visual impairments involves three key components: input, data processing, and output, as depicted in Figure 2. The input section includes three main elements: a sensing unit for detecting environmental conditions, control buttons for system settings, and a power supply module. Data processing is managed by a microcontroller unit (MCU), which interprets input signals and generates appropriate responses. The output system consists of sound and vibration actuators that provide feedback to the user in real time, helping them navigate safely.

A digital compass sensor plays a crucial dual role in the system. First, it detects the swinging motion of the cane—whether from left to right or vice versa. Second, it synchronises the environmental readings from three ultrasonic sensors mounted on the cane. The swinging

motion of the cane is interpreted based on specific angle thresholds. If the detected swing angle is less than 3 degrees, the system assumes the cane is not in active use and remains in standby mode. When the swing angle ranges between 3 and 15 degrees, the system identifies that the cane is being used correctly, prompting the ultrasonic sensors to perform distance measurements and assess spatial conditions. If the swing angle exceeds 15 degrees, the system automatically refreshes the environmental data to ensure the user receives up-to-date spatial information. This dynamic sensing strategy allows the system to respond intelligently to user motion while maintaining energy efficiency and ensuring accurate spatial feedback.

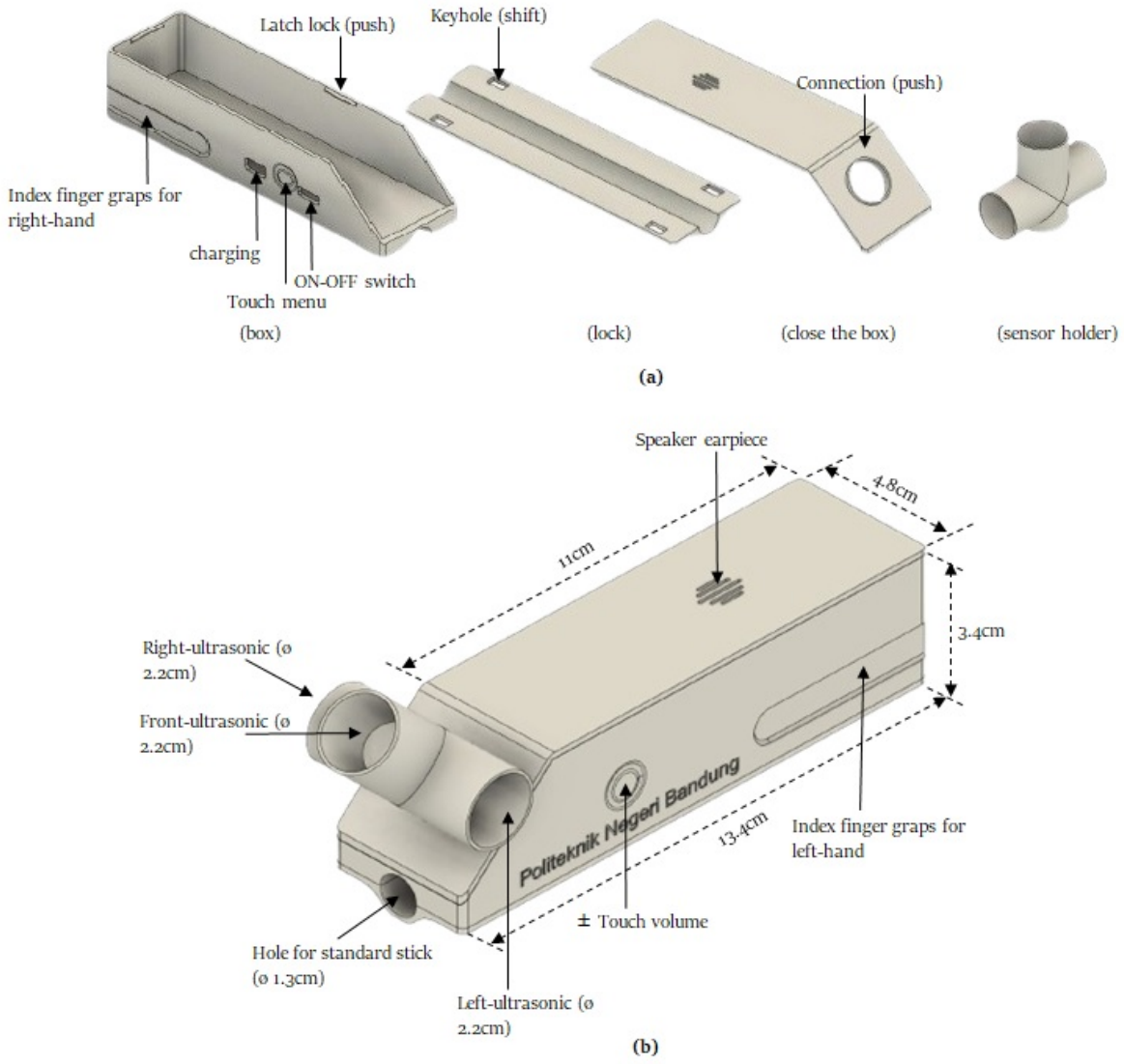

Figure 1 Box Design (a). Parts (b). Combined

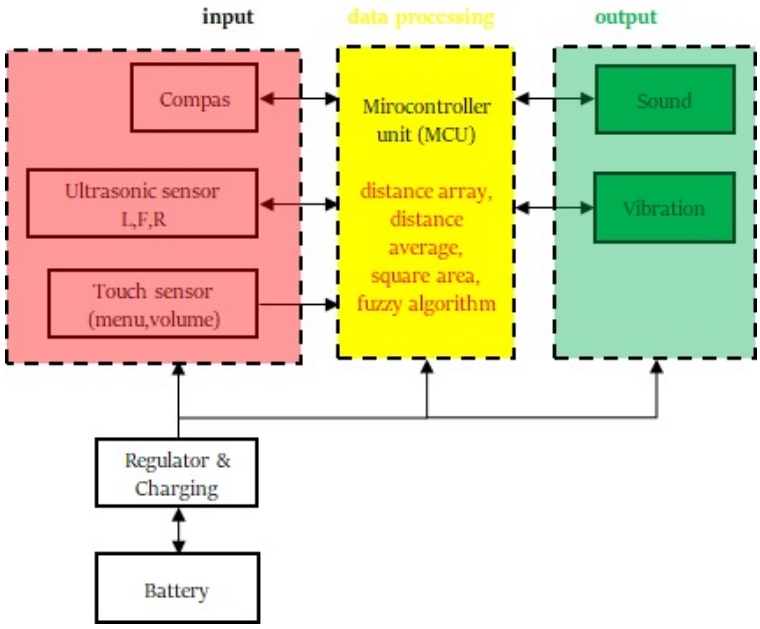

Figure 2 Electronic Hardware Block Diagram

The system features two primary touch-sensitive control buttons: one for menu settings and the other for volume adjustment. The menu button supports four distinct operational modes that configure the output behaviour of the device: Standby Mode (Mode 1), Sound Only (Mode 2), Vibration Only (Mode 3), and Combined Sound and Vibration (Mode 4). Upon initial startup, the device defaults to Standby Mode, in which the actuators remain inactive. When the system is powered on and the menu button is tapped briefly—held for at least one second—it cycles to the Sound Only mode. Subsequent presses allow the user to switch through the other modes in sequence.

The volume control button also offers four settings, but instead of toggling output types, it adjusts the intensity of the sound and vibration feedback. These levels are defined as follows: Mode 1 (Default, Level 15), Mode 2 (Medium, Level 20), Mode 3 (Strong, Level 25), and Mode 4 (Very Strong, Level 30). These numeric values represent the strength of the feedback signal, with higher values corresponding to more intense sound and vibration outputs. A detailed flow of how both the menu and volume settings operate through the touch interface is illustrated in Figure 3.

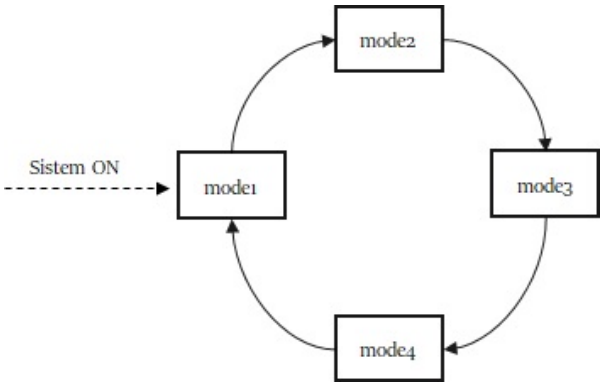

Figure 3 Setting Button Cycle

The primary power source for the electronic system housed within the enclosure is a 3.7V, 1200mAh rechargeable lithium battery. However, since all electronic components operate at a nominal input voltage of 5V DC, the system employs a voltage regulator capable of both step-up and step-down conversion. The step-up configuration raises the battery output to approximately 5V to power the entire electronic circuit, while the step-down path adjusts the voltage to around 4.2V for safe and efficient battery charging. The charging process utilises a standard 5V DC input with a maximum current of 1A, compatible with typical smartphone chargers.

All data processing tasks—including interpreting distance measurements, calculating square-area values, executing fuzzy logic decisions, and integrating information from swing motion, environmental sensing, and user preferences—are handled by a MCU. The system is built on the Arduino Nano platform, utilising the ATMega328 chip as its core processor. The detailed wiring configuration for all electronic components within the system is provided in Table 1.

Table 1 Wiring Configuration

No.	Components	Pin	MCU (Arduino Nano) Pins
1.	Compass	SDA	A4
		SCL	A5
2.	Ultrasonic L	TRIG	D12
		ECHO	D11
3.	Ultrasonic F	TRIG	D10
		ECHO	D9
4.	Ultrasonic R	TRIG	D8
		ECHO	D7
5.	Menu	I/O	D3
6.	Volume	I/O	D2
7.	Sound/beep	O	D6
8.	Vibration/DC motors	O	D5

It is important to note that all Vcc and GND pins of the electronic components and the MCU are first routed through a switch before being connected to the 5V DC power regulator. This ensures centralised power control and allows the system to be turned on or off as needed.

The actuators serve as the output interface that delivers feedback to the user based on detected environmental conditions. In this system, two types of actuators are employed: a buzzer for audible alerts (beeps) and a vibration motor for tactile feedback. Together, these components convey spatial information in real time, enabling users to perceive obstacles or environmental changes through sound and touch.

Software

The data processing software developed in this study integrates multiple computational components, including a movement detection algorithm, distance array analysis, averaging of distance readings, spatial square area calculation, and fuzzy inference using the Sugeno method. The movement detection algorithm plays a critical role in identifying the current state of the cane—whether it is stationary, in motion, or swinging. It also functions as a trigger for activating the fuzzy logic system and ensures synchronisation of distance readings at varying angular positions.

This algorithm operates by comparing the most recent sensor data with the previous reading. The difference is then evaluated against a predefined threshold. If the change exceeds the threshold, the system interprets it as movement; otherwise, it is considered static. In this research, a movement threshold of 3 degrees was established to differentiate between idle and active states.

Once movement is detected—specifically when the cane swings more than 3 degrees—distance array data are collected from three ultrasonic sensors positioned at the left (L), front (F), and right (R) of the cane, as illustrated in Figure 4. A single sweep of the cane across space produces a data package consisting of 30 bytes: 10 bytes for each sensor. These data are then processed to calculate the average distance for each direction, namely the Left Distance Average (LDA), Front Distance Average (FDA), and Right Distance Average (RDA). The resulting average values serve as key inputs for subsequent spatial computation and fuzzy logic analysis.

$$(LDA) = \left\{ \left(\sum_{n=1}^{10} LDn \right)/10 \right\} \quad (1)$$

$$(FDA) = \left\{ \left(\sum_{n=1}^{10} FDn \right)/10 \right\} \quad (2)$$

$$(RDA) = \left\{ \left(\sum_{n=1}^{10} RDn \right)/10 \right\} \quad (3)$$

Equations (1), (2), and (3) show the array data resulting from calculating the average distance for each side of the sensor.

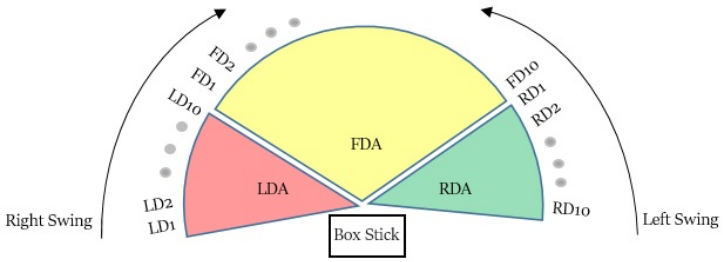

Figure 4 Sensor Average Reading Configuration

The LSSA and RSSA values are as shown in Figure 5. The size of the LSSA value is influenced by the LDA value (x-axis, stick reference point) relative to the FDA value (y-axis). Meanwhile, the RSAA value is influenced by the RDA value (x-axis, stick reference point) on the FDA value (y-axis). The format of the LSSA and RSSA values is as shown in equations (4) and (5).

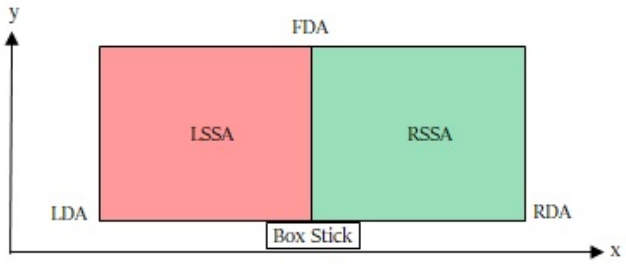

Figure 5 Square Area Reading Configuration

$$(LSSA) = LDA \; x \; FDA \tag{4}$$

$$(RSSA) = RDA \; x \; FDA \tag{5}$$

The fuzzy logic algorithm is designed to interpret input data from ultrasonic sensors and convert it into meaningful output signals that are delivered to the user through actuators—specifically in the form of auditory beeps and tactile vibrations. This decision-making process is carried out through three primary stages: fuzzification, inference, and defuzzification.

During fuzzification, the system transforms raw numerical input values—such as distances measured by the sensors—into linguistic variables. In the inference stage, a rule-based logic framework evaluates these linguistic inputs to determine appropriate responses based on predefined conditions. Finally, in the defuzzification stage, the fuzzy output is converted into a precise control signal that activates the corresponding actuators.

The entire process, from detecting cane swing motion to generating output decisions, is illustrated in detail in Figure 6. This structured approach enables real-time environmental interpretation and responsive feedback, enhancing the user's spatial awareness and mobility.

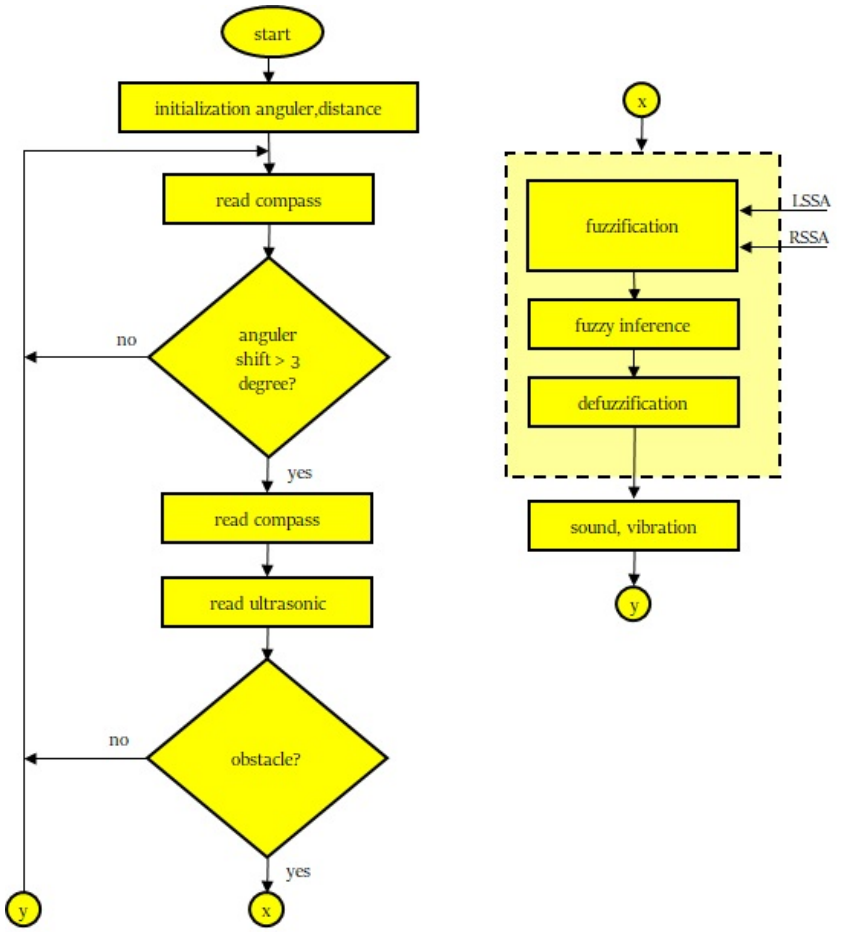

Figure 6 Box and Fuzzy Movement Flow Diagram

The initial phase of the fuzzy algorithm is fuzzification, which involves converting crisp numerical input data into fuzzy sets or linguistic variables, each with an associated degree of membership—commonly referred to as fuzzy input values. The quality and accuracy of this transformation are highly dependent on the design of the input membership functions used in the system.

In this study, the input membership functions are based on square area measurements—specifically the Left Side Square Area (LSSA) and Right-Side Square Area (RSSA). Both inputs follow the same logical structure, as defined in Equation (6). Each of these square area values, expressed in square meters (m^2), is categorised into two linguistic terms: S (Small) and B (Big). The mathematical representations of these membership functions are presented in Equations (7) and (8), and their graphical illustration is shown in Figure 7.

This fuzzification stage is critical for enabling the fuzzy inference engine to process spatial data effectively, allowing the system to interpret environmental conditions and provide intuitive feedback to users through actuators.

$$Left\ and\ Right\ Side\ Square\ Area,\ (LSSA) = (RSSA) = \{S, B\} \quad (6)$$

$$Linguistic\ (S) = \{0, 0, 1.25, 1.5\} \quad (7)$$

$$Linguistic\ (B) = \{1.25,\ 1.5, 4, 4\}) \quad (8)$$

Inference refers to the logical reasoning process applied to fuzzy input values in order to generate fuzzy output values, ultimately forming the basis for decision-making processes (Faisal et al., 2013; Seki & Kuramoto, 2022). At this stage, the system integrates the input membership functions with a predefined set of fuzzy rules to determine the appropriate fuzzy outputs. Each rule is systematically evaluated, and the final decision is derived from the combination and interaction of all applicable rules.

In this study, the Max-Min inference method is employed to assess each fuzzy rule, enabling a straightforward and computationally efficient rule evaluation process. The rule base comprises four fuzzy rules, which have been carefully constructed based on the researcher's insights and practical understanding of the behaviour and dynamics of the cane-mounted electronic module during movement.

These fuzzy rules are formulated in the standard IF-THEN structure, serving as linguistic representations of system behaviour under varying input conditions. An example of such a rule is presented as follows:

Rule1: If x = A1 and y=B1 then Z= C1

Rule 2: If x = A2 and y=B2 then Z= C2

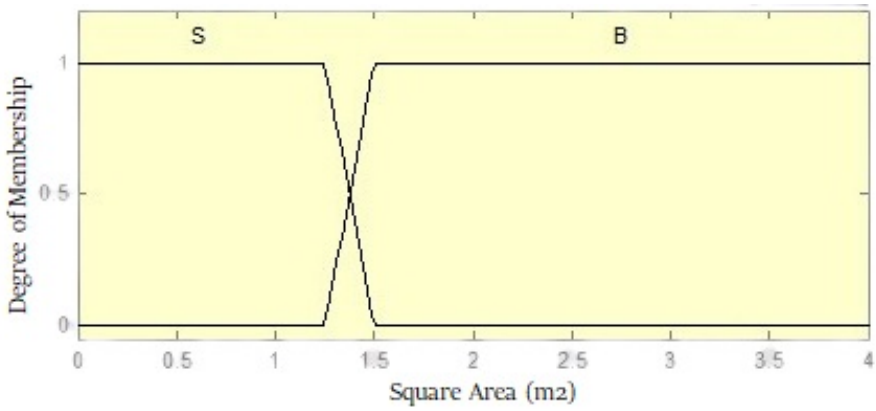

Figure 7 LSSA and RSSA Membership Function Input

The defined fuzzy rules serve to establish the relationship between input variables and the resulting fuzzy output set. In this smart stick system, the linguistic output variables represent navigational directions and constraints, which are foundational in forming the fuzzy decision logic. These output categories include L (Left), NC (No Change—continue moving forward), R (Right), and A (Alarm—indicating that movement in any direction is not permitted). These

linguistic outputs act as actionable decisions based on environmental input data processed through the fuzzy algorithm. The system utilises these outputs to guide user behaviour, enhancing safety and spatial awareness. A complete overview of the four fuzzy rules developed for this application is provided in Table 2, which outlines the rule structures and their corresponding output responses based on input scenarios.

Table 2 Fuzzy Rule Base

No.	Inputs		Outputs
	LSSA	RSSA	
1.	S	S	A
2.	S	B	R
3.	B	S	L
4.	B	B	NC

The defuzzification stage is responsible for transforming fuzzy output values into precise, actionable outputs that can be directly applied to the control system (Omrane et al., 2016). In the proposed system, the Sugeno Weighted Average (WA) method is employed for this conversion process. This technique calculates a crisp output by considering the weighted average of rule outcomes, where each output is assigned a specific constant value. For this design, the output membership values are encoded as pulse constants within the range of -1 to 1. The assigned values are L (Left): -1, NC (No Change): 0, R (Right): 1, and A (Alarm/Alert): 0.5. These values are used to compute the final decision output using the WA method, which is formally expressed in the following formulation.

$$WA = \frac{\alpha 1 z 1 + \alpha 2 z 2 + \ldots + \alpha n z n}{\alpha 1 + \alpha 2 + \ldots + \alpha n} \quad (9)$$

Equation (9) defines αn as the predicate value of the nth fuzzy rule and znz_nzn as the corresponding constant output index. These values are essential in calculating the final crisp output using the Sugeno Weighted Average (WA) defuzzification method. The resulting outputs are delivered to the user through sound (beep) and vibration signals, which are mapped according to the decision made by the fuzzy system. Specifically, a fuzzy output of "L" (Left) triggers two short beeps or two vibration pulses; "R" (Right) triggers one beep or one pulse; "NC" (No Change) results in no output; and "A" (Alarm) produces continuous beeping or vibration. This intuitive output mapping enables the user to quickly interpret directional or alert information during navigation.

Results and Discussion

The testing phase of this research was conducted through both simulation and practical implementation. Simulations were performed using MATLAB software to validate the algorithm and system logic. For real-world evaluation, the electronic hardware system was tested directly in the hallway of Sekolah Luar Biasa Negeri A (SLBN-A) Citeureup, Cimahi. This dual testing approach ensured the system's effectiveness in both controlled and real environmental conditions.

Simulation

The simulation process was conducted to validate that the fuzzy rule base and system design aligned with the intended logic and the designer's conceptual understanding before being translated into code and embedded into the MCU. The fuzzy simulation was developed using MATLAB, with the number of inputs and outputs configured to match the software design specifications, as illustrated in Figure 8.

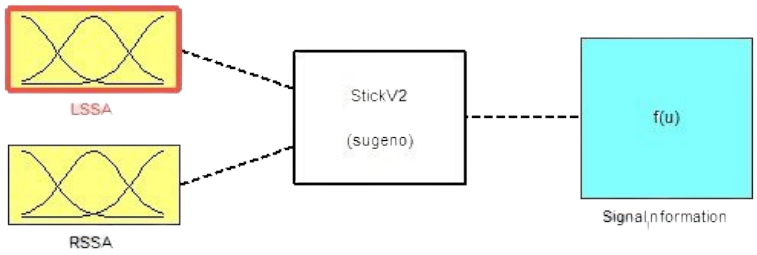

Figure 8 Fuzzy Design – Matlab Simulation

The testing phase was conducted across four distinct scenarios, each designed to represent one of the fuzzy rule bases outlined in Table 2. The first scenario corresponds to a rule where the inputs are LSSA (Small) and RSSA (Small), resulting in an output labelled as X. During this test, square area values ranging from 0 to 200 were applied to both LSSA and RSSA. The result consistently produced a steady output signal with a fuzzy value of X = 0.5, as illustrated in Figure 9.

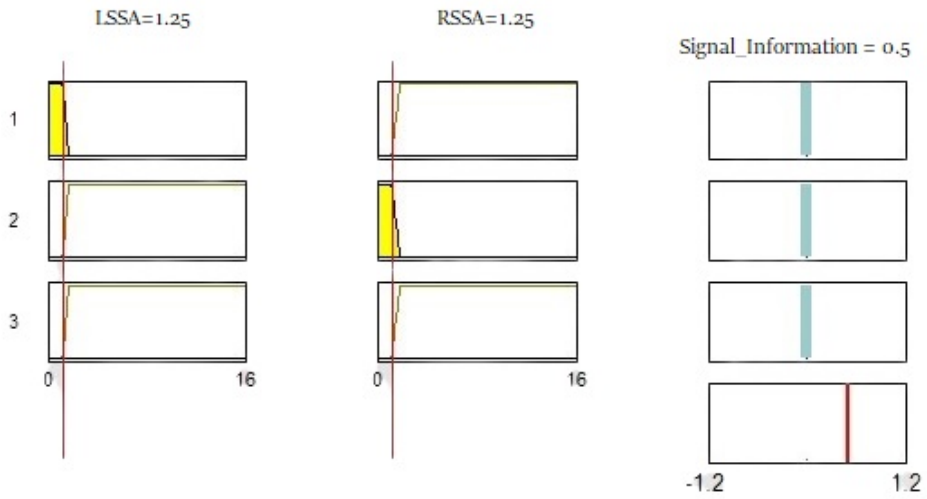

Figure 9 Sample S-S Rule Base Simulation Results

The second testing scenario was designed to evaluate a fuzzy rule base with inputs LSSA (Small) and RSSA (Big), producing an output classified as Right (R). In this test, the square area value assigned to LSSA was set below 1.5, while RSSA was given a value equal to or greater than 1.5. The resulting output was a consistent signal within the fuzzy range of either $0<R<0.50$ or $0.5<R\leq1$.

The third scenario assessed the rule base with inputs LSSA (Big) and RSSA (Small), generating an output identified as Left (L). Here, RSSA was assigned a square area value smaller than 1.5, and LSSA was given a value greater than 1.5. This setup consistently yielded an output signal in the fuzzy range of $-1\leq L<0$.

The fourth scenario tested the rule base with both LSSA and RSSA inputs classified as Big, leading to an output labelled as No Change (NC). The test was conducted by assigning square area values greater than 1.5 to both LSSA and RSSA, which resulted in a stable signal output of NC = 0.

Practice

The evaluation of the standard white cane prototype, enhanced with an integrated electronic system box, was conducted to verify the proper functioning of the fuzzy rule base embedded within the MCU. This testing aimed to ensure that the system operated as expected, in alignment with both the designer's conceptual framework and prior simulation outcomes. The test involved two distinct scenarios, each performed by a different participant with visual impairments. Both individuals are completely blind and serve as employees as well as O&M instructors at SLBN-A Citeureup Cimahi, as shown in Figure 10. Each participant conducted the trial once, navigating a public hall space that lacks specialised infrastructure or guiding tracks for individuals with visual impairments.

(a) (b)

Figure 10 Direct Testing of an Electronic System Prototype by a Individuals with Visual Impairments 10(a) First User 10(b) Second User

In the first trial, depicted in Figure 10a, the user was instructed to navigate using the cane equipped with the electronic system, relying on directional guidance provided through audio (beep) and vibration signals. For this scenario, the user was informed that their initial position faced southeast and was directed to reach a door located at the opposite end of the hall, facing north, as illustrated by the blue trajectory in Figure 11. Table 3 presents the manually recorded test outcomes and measurement data. When the cane detected obstacles, specifically tables 5 and 6, the system activated (positions 3, 4, and 5), generating beeping and vibrating signals at one-second intervals—indicating a command to turn right (R). During segments where no obstacles were detected (positions 6 to 25), no signals were issued (NC), allowing the user to proceed freely and intuitively toward the intended destination. Upon detecting table 7, which lacked a tablecloth and was adjacent to the wall, the system resumed activation (positions 26 and 27), emitting double pulses per second, signalling the user to veer left (L). In this instance, sensor readings were affected by reflections from the wall, as the sensor's position was slightly lower than the tabletop—resulting in the cane making physical contact with the table.

In the second trial, shown in Figure 10b, another user performed the navigation task using the same device but with a different obstacle arrangement and test scenario. This time, the user began facing north and was instructed to proceed forward whenever no guidance signal was present (NC). However, if a directional cue was received, they were required to follow it (either L or R), as indicated by the red path in Figure 11. Table 4 outlines the corresponding test results and manual measurements. At the start of the journey (positions 1–4), the cane detected an obstacle on the right detection area (RDA) more than 2.5 meters away, while the left and right

square sensor areas (LSSA and RSSA) exceeded 4 m². Under these conditions, no alert was triggered (NC), allowing the user to continue forward as planned. When the system detected obstacles such as the stage and table 2 (positions 5–7), it responded with a left-turn signal—beeps and vibrations at two pulses per second—prompting the user to turn left (L). Subsequently, when detecting wall and table 2 from a distance greater than 1.5 meters (positions 8–17), the system remained silent (NC), and the user continued forward in accordance with the instructions.

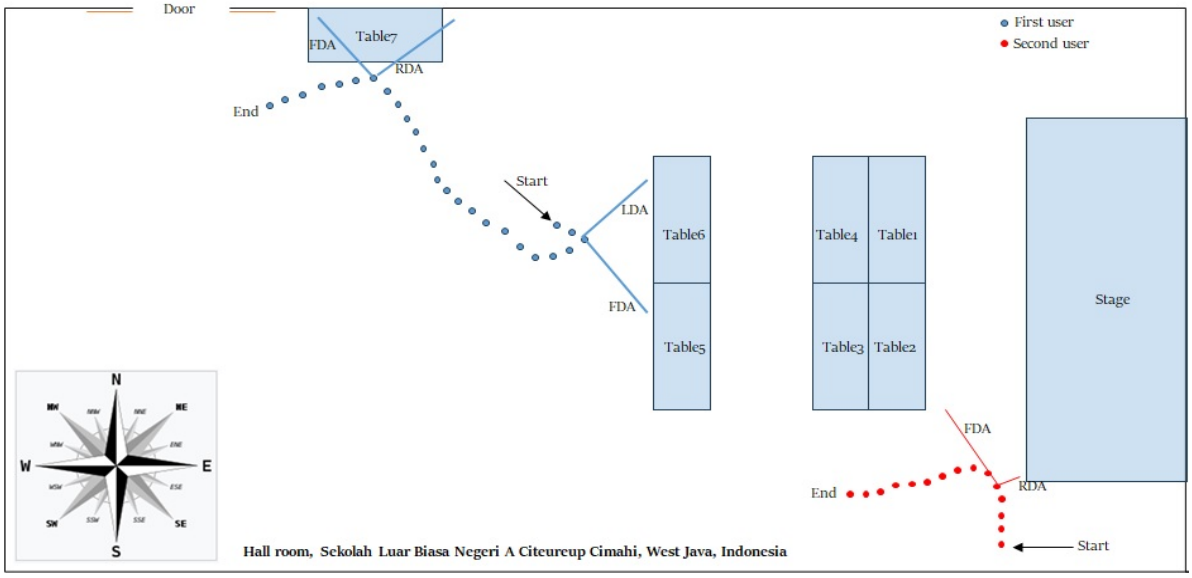

Figure 11 First (Blue) and Second (Red) User Test Results Scenario

Table 3 First User Testing Results Data Per Step

Position to	Distance Average Input (m)			Square Input Area (m2)		Output (Signal Information)	Information
	LDA	FDA	RDAs	LSSA	RSSA		
1-2	>4	1.70	>4	>4	>4	NC	No obstacle detection
3	1	1.4	>4	1.4	>4	R	Left obstacle detection (table 5, 6)
4	0.95	1.5	>4	1.42	>4	R	Left obstacle detection (table 5, 6)
5	0.8	1.8	>4	1.44	>4	R	Left obstacle detection (table 5, 6)
6-25	>4	>4	>4	>4	>4	NC	No obstacle detection
26	>4	1.35	1.1	>4	1.48	L	Right obstacle detection (wall)
27	>4	1.5	1	>4	1.5	L	Right obstacle detection (wall)
28	>4	>4	1.4	>4	>4	NC	No obstacle detection
29	>4	>4	1.5	>4	>4	NC	No obstacle detection

Table 4 Second User Test Results Data Per Step

Position to	Distance Average Input (m)			Square Input Area (m2)		Output (Signal Information)	Information
	LDA	FDA	RDAs	LSSA	RSSA		
1-4	>4	>4	>2.5	>4	>4	NC	Right obstacle detection >2.5
5	>4	>4	0.3	>4	1.2	L	Right obstacle detection (stage)
6	>4	1.4	0.5	>4	0.7	L	Right obstacle detection (stage, table 2)
7	>4	1.3	0.9	>4	1.2	L	Right obstacle detection (stage, table 2)
8-17	>1.5	>4	>1.5	>4	>4	NC	Left-right obstacle detection > 1.5

Conclusions

This study introduces an assistive electronic system mounted on a standard white cane, designed to support the mobility of visually impaired individuals by providing path selection cues through auditory (beeping) and tactile (vibration) signals. The system's functionality was evaluated through both simulation and real-world trials. Practical testing involved two individuals with visual impairments participating in navigating different scenarios within the hall of SLBN-A Citeureup Cimahi. The system identifies environmental conditions using a tri-sensor ultrasonic setup (left, front, and right), which is processed into two square area variables—Left-Side Sensing Area (LSSA) and Right-Side Sensing Area (RSSA)—serving as inputs to a fuzzy logic algorithm. Results from both user trials demonstrate that the system effectively detects obstacles and delivers navigational cues, offering a promising enhancement to traditional orientation methods, such as the eight cardinal directions. The resulting data were analyzed using a confusion matrix approach, yielding perfect classification metrics. Specifically, the system achieved an accuracy of 100%, with sensitivity and specificity also recorded at 100%. These results indicate that the smart cane reliably detects both the presence and absence of obstacles, effectively distinguishing between safe and obstructed paths. Furthermore, the system shows potential for development as a new O&M training approach for individuals with visual impairments. To address limitations in detecting vertically misaligned objects beyond the sensor's range, additional hardware capable of vertical scanning can be incorporated. Moreover, the integration of digital filtering techniques before

the decision-making process may reduce signal disturbances caused by angled obstacle reflections.

Acknowledgements

This research was supported by P3M Politeknik Negeri Bandung through applied scheme funding with contract number B/3.22/PL1.R7/PG.00.03/2024. And representatives of individuals with visual impairments from SLBN-A Citeureup Cimahi who agreed to test.

References

Barontini, F., Catalano, M. G., Pallottino, L., Leporini, B., & Bianchi, M. (2021). Integrating Wearable Haptics and Obstacle Avoidance for the Visually Impaired in Indoor Navigation: A User-Centered Approach. *IEEE Transactions on Haptics, 14*(1), 109-122. https://doi.org/10.1109/TOH.2020.2996748

Bhatlawande, S., Borse, R., Solanke, A., & Shilaskar, S. (2024). A Smart Clothing Approach for Augmenting Mobility of Visually Impaired People. *IEEE Access, 12*, 24659-24671. https://doi.org/10.1109/ACCESS.2024.3364915

Cardillo, E., Li, C., & Caddemi, A. (2022). Millimeter-Wave Radar Cane: A Blind People Aid With Moving Human Recognition Capabilities. *IEEE Journal of Electromagnetics, RF and Microwaves in Medicine and Biology, 6*(2), 204-211. https://doi.org/10.1109/JERM.2021.3117129

Chundury, P., Patnaik, B., Reyazuddin, Y., Tang, C., Lazar, J., & Elmqvist, N. (2022). Towards Understanding Sensory Substitution for Accessible Visualization: An Interview Study. *IEEE Transactions on Visualization and Computer Graphics, 28*(1), 1084-1094. https://doi.org/10.1109/TVCG.2021.3114829

Darlis, A. R., Susana, R., & Sholihah, T. R. (2024). Visible Light-based Outdoor Navigation Systems for Visually Impaired People. *ELKOMIKA: Jurnal Teknik Energi Elektrik, Teknik Telekomunikasi, & Teknik Elektronika, 12*(1). https://doi.org/10.26760/elkomika.v12i1.247

Faisal, M., Hedjar, R., Al Sulaiman, M., & Al-Mutib, K. (2013). Fuzzy Logic Navigation and Obstacle Avoidance by a Mobile Robot in an Unknown Dynamic Environment. *International Journal of Advanced Robotic Systems, 10*(1), 37. https://doi.org/10.5772/54427

Jivrajani, K., Patel, S. K., Parmar, C., Surve, J., Ahmed, K., Bui, F. M., & Al-Zahrani, F. A. (2023). AIoT-Based Smart Stick for Visually Impaired Person. *IEEE Transactions on Instrumentation and Measurement, 72*, 1-11. https://doi.org/10.1109/TIM.2022.3227988

Kementerian Kesehatan Republik Indonesia. (2021). *Katarak Penyebab Terbanyak Gangguan Penglihatan di Indonesia*. Retrieved October 11 from https://kemkes.go.id/eng/%20katarak-penyebab-terbanyak-gangguan-penglihatan-di-indonesia

Kleinberg, D., Yozevitch, R., Abekasis, I., Israel, Y., & Holdengreber, E. (2023). A Haptic Feedback System for Spatial Orientation in the Visually Impaired: A Comprehensive

Approach. *IEEE Sensors Letters, 7*(9), 1-4. https://doi.org/10.1109/LSENS.2023.3307068

Lee, K., Shrivastava, A., & Kacorri, H. (2023). Leveraging Hand-Object Interactions in Assistive Egocentric Vision. *IEEE Transactions on Pattern Analysis and Machine Intelligence, 45*(6), 6820-6831. https://doi.org/10.1109/TPAMI.2021.3123303

Masud, U., Saeed, T., Malaikah, H. M., Islam, F. U., & Abbas, G. (2022). Smart Assistive System for Visually Impaired People Obstruction Avoidance Through Object Detection and Classification. *IEEE Access, 10*, 13428-13441. https://doi.org/10.1109/ACCESS.2022.3146320

Ogedengbe, T. O., Kreidy, C., Gürke, N., Twahirwa, B. N., Boateng, M. A., Eslahi, M., Khodayari, F., Nemargut, J. P., Martiniello, N., & Wittich, W. (2025). Feasibility of telerehabilitation to address the orientation and mobility needs of individuals with visual impairment: perspectives of current guide dog users. *Disability and Rehabilitation, 47*(5), 1298-1308. https://doi.org/10.1080/09638288.2024.2368058

Omrane, H., Masmoudi, M. S., & Masmoudi, M. (2016). Fuzzy Logic Based Control for Autonomous Mobile Robot Navigation. *Comput Intell Neurosci, 2016*, 9548482. https://doi.org/10.1155/2016/9548482

Organization, W. H. (2024). *Blindness and vision impairment*. Retrieved October 3 from https://www.who.int/news-room/fact-sheets/detail/blindness-and-visual-impairment

Qiu, S., Hu, J., Han, T., Osawa, H., & Rauterberg, M. (2020). An Evaluation of a Wearable Assistive Device for Augmenting Social Interactions. *IEEE Access, 8*, 164661-164677. https://doi.org/10.1109/ACCESS.2020.3022425

Seki, H., & Kuramoto, T. (2022). Fuzzy Inference-Based Driving Control System for Pushrim-Activated Power-Assisted Wheelchairs Considering User Characteristics. *IEEE Transactions on Human-Machine Systems, 52*(5), 1049-1059. https://doi.org/10.1109/THMS.2022.3195890

Supriyadi, T., Salsabila, A., Solihin, R., Hanifatunnisa, R., Setiadi, B., & Afni, S. (2021, 2021/11/23). Position Coordination Aid for Blind Persons Based on LoRa Point to Point. Proceedings of the 2nd International Seminar of Science and Applied Technology (ISSAT 2021),

Supriyadi, T., Solihin, R., Habinuddin, E., & Sudrajat, S. (2024, 01/29). Development of Fuzzy Algorithm as Mobility Aid for Blind Person Using Two Sensor Points: Visual Aid for Blind Person. *International Journal of Engineering Continuity, 3*(2), 132-146. https://doi.org/10.58291/ijec.v3i2.336

Tanabe, T., Fujimoto, Y., Nunokawa, K., Doi, K., & Ino, S. (2023). White Cane-Type Holdable Device Using Illusory Pulling Cues for Orientation & Mobility Training. *IEEE Access, 11*, 28706-28714. https://doi.org/10.1109/ACCESS.2023.3259965

Tian, S., Zheng, M., Zou, W., Li, X., & Zhang, L. (2021). Dynamic Crosswalk Scene Understanding for the Visually Impaired. *IEEE transactions on neural systems and rehabilitation engineering, 29*, 1478-1486. https://doi.org/10.1109/TNSRE.2021.3096379

Zhang, L., Jia, K., Liu, J., Wang, G., & Huang, W. (2023). Design of Blind Guiding Robot Based on Speed Adaptation and Visual Recognition. *IEEE Access, 11*, 75971-75978. https://doi.org/10.1109/ACCESS.2023.3296066